Fitting psychometric functions to achromatic brightness matching data

Joris Vincent

A thesis submitted
in partial fulfillment to the requirements
for the degree of

Master of Science

University of Washington

2017

Reading Committee:

Steven L. Buck, Chair

Geoffrey M. Boynton

Program Authorized to Offer Degree:
Psychology

University of Washington

Abstract

Fitting psychometric functions to achromatic brightness matching data

Joris Vincent

Chair of the Supervisory Committee:
Dr. Steven L. Buck
Psychology

In asymmetric brightness matching procedure, one of two target regions is set by the experimenter at a fixed luminance (the *reference*). This reference, with its fixed luminance and fixed relationship to the surrounding context will be perceived by the participant at some brightness. The participant then adjusts another target region (the *match*), until it is perceived as equally bright. If the context has no influence on the perception of brightness of either the reference and the matching target, then the only way to match the two target regions would be to set the match at the same physical luminance as the reference. Any difference in physical luminance of the two targets at match, is a measure of the magnitude of the brightness induction effect of the surrounding context. However, this induction magnitude seems to be depend on the luminance relationships not just between the targets, but also between the target luminance and the surround context luminances. The current investigation aims to develop descriptive models of asymmetric matching data, that can adequately summarize the induction magnitude over a range of target luminance values.

TABLE OF CONTENTS

LIST OF FIGURES

LIST OF TABLES

Chapter 1

BRIGHTNESS MATCHING

Human perception of brightness is not veridical with physical photometric luminance (Kaiser, 1971). Instead, a stimulus embedded in a surrounding context can be made to look brighter or darker than an identical stimulus in a different context (Kingdom, 2011). Generally, such brightness induction effects are considered to aid in keeping the perception of surface reflectance (*lightness*) constant across changes in illumination (Kingdom, 2011). A variety of mechanisms for brightness induction have been proposed, for a variety of different induction effects, such as lateral inhibition between neural units with neighboring receptive fields (Jameson & Hurvich, 1975; Moulden & Kingdom, 1989; Kingdom, 2011), responses by units with large receptive fields blending luminance values of subthreshold stimuli (Helson & Rohles, 1959; Helson, 1963), additional normalization or inhibition of the aforementioned neural units (White, 1981; White & White, 1985; Moulden & Kingdom, 1989; Blakeslee & McCourt, 1999; Robinson, Hammon, & de Sa, 2007), perceptual grouping on the basis of Gestalt principles (A. L. Gilchrist et al., 1999; A. Gilchrist, 2015; A. L. Gilchrist, 2015), on the basis of geometric features such as edges (Rudd & Arrington, 2001; Rudd, 2013) and T-junctions (Zaidi, Spehar, & Shy, 1997; Todorović, 1997, 2010; Anderson, 1997), and perceptual scission into causal layers, possible with inferences about transparency or lighting conditions (Anderson, 1997, 2001, 2003; Anderson & Winawer, 2005).

The processes and mechanisms underlying brightness perception are often studied using brightness illusions, such as the one by White (1979), show in Figure 1.1. In this classic illusion consists of a square-wave grating with one (set of) target elements replacing parts of the white bars of the grating (i.e in phase with the grating) and another (set of) target elements replacing parts of the black bars of the grating (i.e. in counter-phase with the

grating), as depicted in Figure 1.1. The bars that the target elements partially replace are dubbed collinear with the target, while the other bars of the grating are dubbed the flanking bars. Generally, observers perceive the targets flanked by the white bars as brighter than the equiluminant target elements flanked by the black bars.

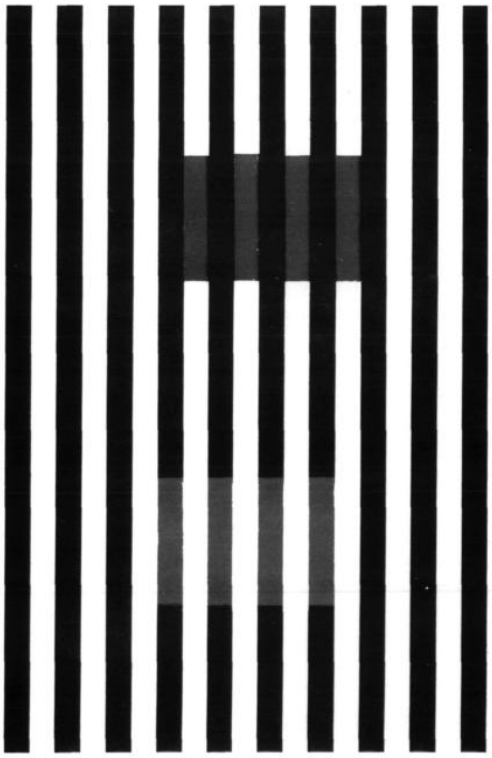

Figure 1.1: **White's illusion**, from White (1979). The two sets of gray target elements are physically identical, yet the upper set (coaxial with the white bars) appears darker than the lower set (coaxial with the black bars).

1.1 Asymmetric brightness matching

Quantitatively, the strength of an illusion such as White (1979) classic illusion can be done through asymmetric brightness matching. In this procedure, one of the two target regions is set by the experimenter at a fixed luminance (the *reference*). This reference, with its fixed luminance and fixed relationship to the surrounding context will be perceived by the partic-

ipant at some brightness. The participant then adjusts the other target region (the *match*), until it is perceived as equally bright. If the context has no influence on the perception of brightness of either the reference and the matching target, then the only way to match the two target regions would be to set the match at the same physical luminance as the reference. Any deviation from this null hypothesis, indicates that the surrounding context influences the perceived brightness of either (or both) target. Moreover, the difference in physical luminance necessary to achieve a perceptual brightness match can be considered the luminance difference that creates an equivalent brightness difference as the target. In other words, the difference in physical luminance of the two targets at match, is a measure of the magnitude of the brightness induction effect of the surrounding context. However, this induction magnitude seems to be depend on the luminance relationships not just between the targets, but also between the target luminance and the surround context luminances. For instance, the effect in White (1979) illusion is not present when both targets are brighter than the white elements in the surround (Spehar, Gilchrist, & Arend, 1995; Spehar, Clifford, & Agostini, 2002). The current investigation aims to develop descriptive models of asymmetric matching data, that can adequately summarize the induction magnitude over a range of target luminance values.

This asymmetric brightness matching does not provide a measure of the brightness of each target; instead, the difference in physical luminance at match is a measure of the brightness difference between the targets as a result of the surrounding context. An outstanding question in investigations of White's illusion is whether this difference is due to darkening of one target, or brightening of the other target, or both. The present investigation will not attempt to answer this question, but attempts only to measure and model the brightness induction effect generated by the different stimuli.

1.2 Brightness matching data collection

In the current investigation, an asymmetric brightness matching task was employed to measure the brightness induction effect. To measure brightness in isolation of any chromatic

effects, both targets were kept achromatic (CIE 1964 10° x = .33, y = .33; L/(L+M) cone ratio = .66, S/(L+M) cone ratio = .0032). On every trial, one target, the reference, was kept at a fixed luminance, pseudo-randomly drawn from the uniform integer distribution between 1 cd/m^2 and 90 cd/m^2. Participants adjusted the physical luminance of the other target, the match, until it matched the reference in brightness. Participants could not adjust the chromaticity of the match target. Each session of the brightness matching task consisted of 50 trials, during which the side of the reference was counterbalanced, so that 25 trials had the reference on the left side.

Even at a brightness match, the two targets might differ in their perceived lightness, albedo, shading or transparency. Participants were instructed to match the two targets on brightness, and told that even at the best possible setting, the match and reference might not look identical. To find the best possible match, participants were to find an initial setting that they perceived as a match, then move the light level away from this setting by a few steps, and try to find their original setting again.

1.2.1 Procedure

All stimuli were presented on a ViewSonic G90fB (Model No. VS 10794) 19 inch (48.3 cm) CRT monitor, using custom routines written for MATLAB (Mathworks, 2016) and Psychtoolbox (Brainard, 1997). The gamma lookup table in the system was replaced with a linearized gamma table, calculated from luminance and chromaticity measurements by a Spectrascan PR 705 photometer. To reduce adaptation effects, the stimulus display cycled continuously on (1 s) and off (3 s), replaced by a full 32° x 24° achromatic field at 48 cd/m^2. When the stimulus was not presented, a fixation cross appeared in the center of the display. In an otherwise dark room, participants viewed the stimulus binocularly through natural pupils from a chin rest at approximately 63 cm distance from the screen.

A total of 25 participants set achromatic brightness matches for either 1 stimulus (N = 17), 2 stimuli (N = 6) or all three stimuli (N = 2). All participants were undergraduate Psychology students (XX male, XX female) at the University of Washington, compensated

for their participation with course credit. The sample is representative of the UW undergraduate population, which is largely of Caucasian and East-Asian heritage. All participants were screened for color vision deficiency using the Ishihara pseudo-isochromatic plates; one participant (initials AGP) was a deuteranope, all other participants were color normal. All participants had normal or corrected-to-normal spatial vision.

Participants adjusted the luminance using two keys on a keyboard. When satisfied with their setting, participants would accept their setting with another keypress, and a new trial would appear. Fixation was not enforced, but participants were encouraged to accept settings only while fixating on the center of the display, as indicated by the fixation cross during the 3s off-cycle. Participants completed one session of achromatic matching at a time (approx. 45 minutes), and a maximum of one session per day.

1.2.2 Stimuli

Three stimuli were used to investigate models of the relationship between target luminance and brightness induction magnitude by a surround context: a version of Whites classic illusion, a checkerboard variant, and set of concentric rings. Each stimulus consists of an articulated high-contrast surround context that induces a brightness difference in two targets. The three stimuli were tested in separate experiments.

White's illusion

In the current investigation, a horizontally oriented square-wave grating of approximately 0.40 cpd surrounded two sets of 3 target elements each. The white phase of the grating was achromatic (1931 CIE x = .33, y = .33; L/(L+M) cone ratio = .66, S/(L+M) cone ratio = .0032) at a constant 95 cd/m^2. The black phase of the grating was <0.001 cd/m^2. The total display subtended 32° x 24° visual angle.

On the left hand side of the display, the target elements were in phase with the surround grating, partly replacing the white bars. On the right hand side, the target elements were in complete counterphase with the surround grating, partly replacing the black bars. The

target elements were centered at 5.5° horizontal eccentricity, 5° in width, and spanning approximately 7.5° degrees vertically (3 full cycles).

Checkerboard variant

In the current investigation, a 20 x 10 checkerboard of 0.5° square checks subtended 10° x 5° of the visual field. The white checks were achromatic (CIE 1964 10° x = .33, y = .33; L/(L+M) cone ratio = .66, S/(L+M) cone ratio = .0032) at a constant 95 cd/m^2, the black checks at <0.001 cd/m^2. The checkerboard was placed on a 24° x 16° achromatic background at 48 cd/m^2. On the left hand side of the display, the target replaced 8 white checks of the display in a 2° x 2° region. On the right hand side of the display, the target replaced 8 black checks of the display. Both targets were centered at 2.5° horizontal eccentricity.

Radial variant

In the current investigation, two sets of 7 concentric rings were placed on a 24° x 16° achromatic background at 48°, centered at 2° horizontal eccentricity each. The width of each ring was 0.125°, including the inner circle of the display. Each entire set of rings was 2° in diameter. Alternatively, each set of concentric rings can be considered to be a radial square-wave grating with a frequency of 8 cpd. The white rings were achromatic (CIE 1964 10° x = .33, y = .33; L/(L+M) cone ratio = .66, S/(L+M) cone ratio = .0032) at a constant 95 cd/m^2, the black rings at <0.001 cd/m^2.

The target elements were the middle (4th) ring in each set. Unlike the other two stimuli, this radial variant of Whites illusion requires two separate gratings, each containing one full target ring. The two displays differ in their phase: the inner ring of the left display is black, while the inner ring of the right display is white. The target ring in the left display replaces a white ring, and is contiguous with two black rings; the target ring in the right display replaces a black ring, and is contiguous with two white rings.

Chapter 2
LINEAR MODEL

The simplest family of models that could fit the achromatic brightness matching data, would be linear models. In such a model, the left target luminance at match would be a linear transformation of the right target luminance at match. One such linear transformation would be an additive shift: the left target luminance at match would be a fixed (per participant, per stimulus) number of candelas higher than the right target at match, i.e., equation 2.1. An additive model would be applicable if the surround context influenced the target brightnesses by a fixed amount, regardless of the luminances of the targets.

$$Lum_{left} = Lum_{right} + b \tag{2.1}$$

Another linear transformation that could be applied, is a scaling: the left target luminance at match would be scaled from the right target at match, i.e., equation 2.2. 2.2. A scaling model would be applicable if the surround context influenced the target brightnesses dependent on the luminance of the targets, but keeping their relative brightness constant.

$$Lum_{left} = a * Lum_{right} \tag{2.2}$$

These two transformations could also be combined, such that the left target luminance at match is both scaled and shifted compared to the right target luminance at match. i.e., equation 2.3.

$$Lum_{left} = a * Lum_{right} + b \tag{2.3}$$

Figure 2.1 shows the results of fitting each of these three models to the achromatic brightness matching data of participant AGP on the classic illusion. The scatterplots show the brightness matching data, with the right target luminance on the horizontal axis, the left

target luminance on the vertical axis. Each dot represents the luminances of the two targets at match during one trial. If perceived brightness was solely a function of target luminance, and not context, the two target patches should be perceived as equally bright only when both have have the same physical luminance, regardless of what that luminance is. Each trial would then fall on the unity line (dashed in Figure **??**), indicating equiluminance. The trials do not fall on the equiluminant line; perceived equal brightness is reached when the target patches have different luminances. This difference in luminance necessary to create matching brightness in the target patches is smallest when both target patches are very dim or very bright. In particular, the difference in luminance is minimal when the luminance of the reference target approaches the luminance of either the black or white elements of the background grating. This bounding of the brightness difference could be due to either the reference or the target patch being indistinguishable from the elements it is embedded in, and has been previously reported (Spehar et al., 1995).

The black line in each plot indicates the model prediction. Models were fit by finding the parameter values for a best-fit in the least-squares sense; the bar graph in Figure 2.1D shows the goodness-of-fit of each model expressed as R^2. The variability inherently present in the data limit the performance of any model, so as a comparison, the split-half reliability of the data is presented in 2.1D. The achromatic brightness matching data was randomly split into a "training" and "testing" half, and the left target luminances of each trial in the testing half was predicted as the mean left target luminance of all trials in the training half with the same right target luminance.

For this exemplar, an additive shift of $10.50\,\mathrm{cd/m^2}$ accurately captures the data ($R^2 = .96$), as accurate as the split-half reliability ($R^2 = .96$). The best-fitting scaling of 1.18 does notably worse, $R^2 = .92$. The combined linear model performs as well as the additive shift ($R^2 = .96$). The best-fitting parameters of the combined linear model show that the model relies mainly on the additive shift ($10.21\,\mathrm{cd/m^2}$ in the combined model), and barely on the scalar (1.01 in the combined model). Since the combined model contains an extra parameter, compared to the other two models, a better fit for the combined model could be spurious;

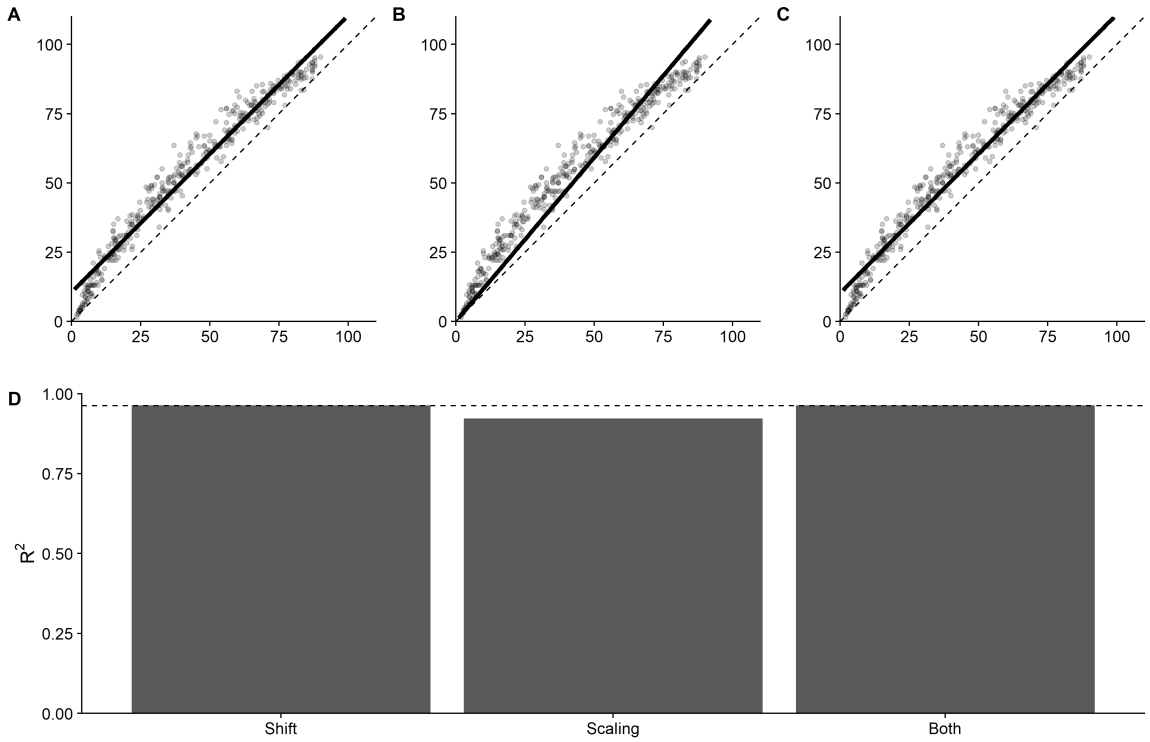

Figure 2.1: **Linear model fits** to the example data from participant AGP on the Classic illusion. **A** Left target luminance is a linear translation (shift by additive constant) of the right target luminance. **B** Left target luminance is a linear scaling of the right target luminance. **C** Left target luminance is a linear transformation of right target luminance that consists of both a translation and a scaling. **D** Goodness-of-fit, expressed as R^2, of the three models to the exemplar data, compared to the split-half reliability (dotted line).

this model can always fit the data better than either of the two restricted models. An F-test can be used test if the additional parameter has significant explanatory value, based on the residual sum of squares (RSS) and number of parameters (p) of the unrestricted (2) and restricted model (1), i.e., equation 2.4.

$$F = \frac{\left(\frac{RSS_1 - RSS_2}{p_2 - p_1}\right)}{\left(\frac{RSS_2}{n - p_2}\right)}, withdf = (p_2 - p_1, n - p_2) \tag{2.4}$$

$$F = \frac{RSS_1 - RSS_{Combined}}{\left(\frac{RSS_{Combined}}{n-2}\right)}, withdf = (1, n-2) \tag{2.5}$$

For the linear models, this reduces to equation 2.5. In the case of the exemplar data, the combined model is a significant improvement over the simple scaling ($F(1,398) = 442.76$, $p < .0001$), but not over the additive shift ($F(1,398) = 442.76$, $p = .49$). Together, this suggests that the exemplar data can be accurately described as linear additive shift in the luminances of the two targets at match, without the need for an additional scaling parameter.

Table 2.1: **Linear model fits on the Classic illusion** for all participants. Scalar and shift terms in the combined models that provide a significant improvment are bolded.

	Reliability	Shift		Scaling		Both		
Participant	R^2	Shift	R^2	Scalar	R^2	Scalar	Shift	R^2
AGP	.96	10.50	.96	1.18	.92	1.01	10.21	.96
AMC	.95	12.43	.95	1.21	.91	1.02	11.57	.95
AYU	.04	-3.76	.24	0.84	.33	**0.61**	**14.04**	**.40**
KXW	.91	9.76	.93	1.18	.91	**1.03**	**8.48**	**.94**
MJK	.89	10.50	.92	1.15	.84	**0.92**	**13.92**	**.93**
NDJ	.82	11.33	.87	1.19	.80	**0.96**	**13.01**	**.87**
QXY	.94	19.51	.93	1.34	.82	**1.04**	**17.95**	**.93**
RAM	.60	13.70	.73	1.21	.58	**0.87**	**18.85**	**.74**
RXN	.94	7.36	.97	1.13	.96	**1.04**	**5.60**	**.97**
SXF	.94	11.32	.95	1.19	.91	1.01	10.69	**.95**
VXL	.95	8.10	.96	1.11	.91	**0.92**	**11.56**	**.97**
YPW	.93	12.23	.94	1.21	.89	**1.03**	**10.93**	**.94**
Mean	**.81**	**10.25**	**.86**	**1.16**	**.81**	**0.95**	**12.24**	**.88**

Table 2.1 reports the best-fitting parameters, in the least-squares sense, and corresponding goodness-of-fit, expressed as R^2 for each model and participant on the Classic illusion. The same pattern for the exemplar data can be seen for most participants: an additive shift and combined model describe the data accurately (mean $R^2 = .86$, and .88, respectively), and better than a scalar (mean $R^2 = .81$). The combined model relies mainly on an additive shift (mean = $12.24\,\mathrm{cd/m^2}$) comparable to that of the best-fitting additive shift in

isolation (mean = 10.25 cd/m^2), and relies very little on the scaling term (mean = 0.95). For most participants, however, the scalar term does have explanatory power, as the combined model predicts the matches significantly better than the translation term alone (all combined models outperform the scalar term alone).

Table 2.2: **Linear model fits on the Checkerboard variant** for all participants. Scalar and shift terms in the combined models that provide a significant improvment are bolded.

	Reliability	Shift		Scaling		Both		
Participant	R^2	Shift	R^2	Scalar	R^2	Scalar	Shift	R^2
APF	0.53	-2.05	0.12	0.85	0.22	**0.54**	**18.83**	**0.38**
DDS	0.87	-7.26	0.75	0.85	0.78	**0.84**	0.55	**0.78**
JCW	0.87	-17.03	0.76	0.71	0.79	**0.81**	**-6.68**	**0.80**
MAW	0.88	-6.53	0.77	0.85	0.82	**0.80**	**3.33**	**0.82**
MMT	0.91	4.93	0.85	1.04	0.82	**0.86**	**10.96**	**0.87**
MSS	0.80	7.55	0.66	1.06	0.57	**0.75**	**18.49**	**0.74**
RXN	0.92	-0.92	0.91	0.97	0.91	**0.94**	**2.07**	**0.91**
SMK	0.77	6.54	0.57	1.03	0.50	**0.73**	**17.99**	**0.67**
TCW	0.91	1.44	0.82	1.00	0.82	**0.89**	**6.46**	**0.83**
XTL	0.73	-2.63	0.68	0.93	0.69	**0.88**	**2.72**	**0.69**
YPW	0.79	8.03	0.71	1.09	0.62	**0.79**	**17.25**	**0.76**
Mean	**0.81**	**-0.72**	**0.69**	**0.94**	**0.68**	**0.80**	**8.36**	**0.75**

Table 2.2 reports the best-fitting parameters, in the least-squares sense, and corresponding goodness-of-fit, expressed as R^2 for each model and participant on the Checkerboard variant. The Checkerboard variant shows a subtly different pattern of model fits as the Classic illusion: an additive shift and combined model describe the data accurately (mean R^2 = .69, and .75, respectively), and better than a scalar (mean R^2 = .68). The combined model does rely on an additive term (mean = 8.36 cd/m^2) for a significant improvement over the scaling, for all but one participant (DDS). However, this additive term is generally very different in direction and magnitude from the additive shift in the restricted model (mean

$= -0.72\,\mathrm{cd/m^2}$). Instead, for all participants, the combined model relies also on the scaling term (mean = 0.80) for a significant improvement over the additive shift model. Thus, the brightness matches on the checkerboard variant can be best explained by a linear model containing both an additive term and a scaling.

Table 2.3: **Linear model fits on the Radial variant** for all participants. Scalar and shift terms in the combined models that provide a significant improvement are bolded.

	Reliability	Shift		Scaling		Both		
Participant	R^2	Shift	R^2	Scalar	R^2	Scalar	Shift	R^2
AMC	0.46	17.12	0.39	1.21	-0.02	**0.65**	**30.54**	**0.54**
GAL	0.92	18.13	0.76	1.31	0.50	**0.87**	**23.18**	**0.77**
JCW	0.89	-9.44	0.86	0.82	0.87	**0.87**	**-3.05**	**0.88**
MAW	0.92	0.40	0.86	0.97	0.86	**0.86**	**7.13**	**0.88**
MMT	0.92	11.12	0.83	1.15	0.72	**0.87**	**16.67**	**0.85**
MRM	0.93	-2.66	0.82	0.90	0.87	**0.78**	**8.11**	**0.90**
MSS	0.67	17.87	0.40	1.25	0.03	**0.69**	**29.06**	**0.49**
RXN	0.84	2.19	0.68	0.96	0.68	**0.73**	**14.44**	**0.80**
SCR	0.92	17.06	0.77	1.26	0.48	**0.83**	**23.21**	**0.80**
SRS	0.93	28.03	0.78	1.57	0.47	1.04	**26.61**	**0.78**
XTL	0.66	5.60	0.49	1.05	0.44	**0.76**	**16.31**	**0.54**
YPW	0.79	14.96	0.65	1.24	0.44	**0.83**	**21.17**	**0.68**
Mean	**0.82**	**10.03**	**0.69**	**1.14**	**0.53**	**0.81**	**17.78**	**0.74**

Table 2.3 reports the best-fitting parameters, in the least-squares sense, and corresponding goodness-of-fit, expressed as R^2 for each model and participant on the Radial variant. The Radial variant shows a pattern that corresponds to that for that Classic illusion in broad strokes: an additive shift and combined model describe the data accurately (mean $R^2 = .69$, and .74, respectively), and better than a scalar (mean $R^2 = .53$). The combined model does rely on an additive term (mean $= 17.78\,\mathrm{cd/m^2}$) for a significant improvement over the scaling, for all participants. Like on the Classic illusion, and in contrast to the

Checkerboard variant, this additive term is generally in the same direction as the additive shift in the restricted model (mean = 10.03 $\mathrm{cd/m^2}$). In contrast to the Classic illusion, and in line with Checkerboard variant, for all but one participant, the combined model relies also on the scaling term (mean = 0.81) for a significant improvement over the additive shift model. Thus, the brightness matches on the Radial variant can be best explained by a linear model containing both an additive term and a scaling.

Chapter 3

LUMINANCE RESPONSE FUNCTION (LRF)

While the linear models can capture the overall trend of the achromatic brightness matching data in terms of direction and magnitude of induction, Figure 2.1A&C reveal a shortcoming of these models. Their linear nature requires the predicted luminance to fall along a straight line; the data, however, is better described as a curve. At extreme luminances, nearing the lowest or the highest luminance in the display, the induction effect is weaker than at intermediate luminances. The linear models seem to capture the induction effect at these intermediate levels, but as a result overestimate the effect at the extreme luminances. This is not a trivial limitation of the linear models: while indeed most of the luminances tested fall in the intermediate range that these models can describe well, the fact that the induction effect seems to be bounded by the luminances of the inducing context is certainly of theoretical relevance to explanations of White's illusion.

To overcome this limitation of linear models, and attempt to capture the full curve of the brightness matching data, a nonlinear model must be applied. To construct a model of achromatic brightness matching, it is worthwhile to first consider the relationship between physical luminance and perceived brightness for a single stimulus. Naka and Rushton (1966) first characterized the responses of retinal cells to light contrast using the equation that has come to bear their name since, equation 3.1. This sigmoidal function can be used to describe the relationship between some contrast C, and a neural response R (usually in terms of spike rate).

$$R(C) = R_{max}\frac{C^p}{C^p + \sigma^p} + b \tag{3.1}$$

The R_{max} parameter is a scaling factor that determines the maximal response: as the contrast increases, the R asymptotically approaches R_{max} and the response thus saturates. The

parameter σ determines the contrast level at which R is at half its asymptotic maximum, and is thus referred to as the *semi-saturation constant*. While the Naka-Rushton equation is most often applied as a contrast response function, charactarizing a neurons or systems response R to contrast C, it can serve a purpose in the current investigation as the basis for a Luminance Response Function (LRF). Equation 3.2 describes the relationship between the luminance of a stimulus, and its perceived brightness with the same shape as the Naka-Rushton equation.

$$Brightness(Lum) = \alpha \frac{Lum^{p+q}}{Lum^p + \sigma^p} + b \tag{3.2}$$

One addition to the LRF in 3.2 is the parameter q, which prevents the LRF from saturating. There is no reason to assume that perceived brightness would saturate over the luminance ranges tested in the current investigation. Another aspect of the LRF to note is that perceived brightness here is in arbitrary units, since there are no physical units to measure perceived brightness in (without comparison to another stimulus).

3.1 Matching LRFs

A single LRF describes the relationship between physical luminance and the perceived brightness of a single stimulus. By combining two LRFs, one can describe the relationship between the two targets. Defining an LRF for the right target allow for a prediction to be made about the perceived brightness of the right target at any physical luminance, e.g., $50\,\mathrm{cd/m^2}$ (Figure 3.1, red arrow). This predicted brightness can then be applied to the LRF for the left target (Figure 3.1, purple arrow). That LRF allows then gives a physical luminance value for the left target, e.g., $64.2\,\mathrm{cd/m^2}$ (Figure 3.1, blue arrow), at which the LRF for the left target would predict that same perceived brightness. Thus, the combination of the two LRFs allows one to predict the a luminance of the left target, that would predict the same perceived brightness as a known luminance of the right target. Note that this calculation has the same logic as the psychophysical achromatic brightness matching paradigm: one target is fixed at a known luminance, and it generates some perceived brightness. This brightness is hard to quantify perceptually; in the model, it is in arbitrary units. Yet, adjusting another

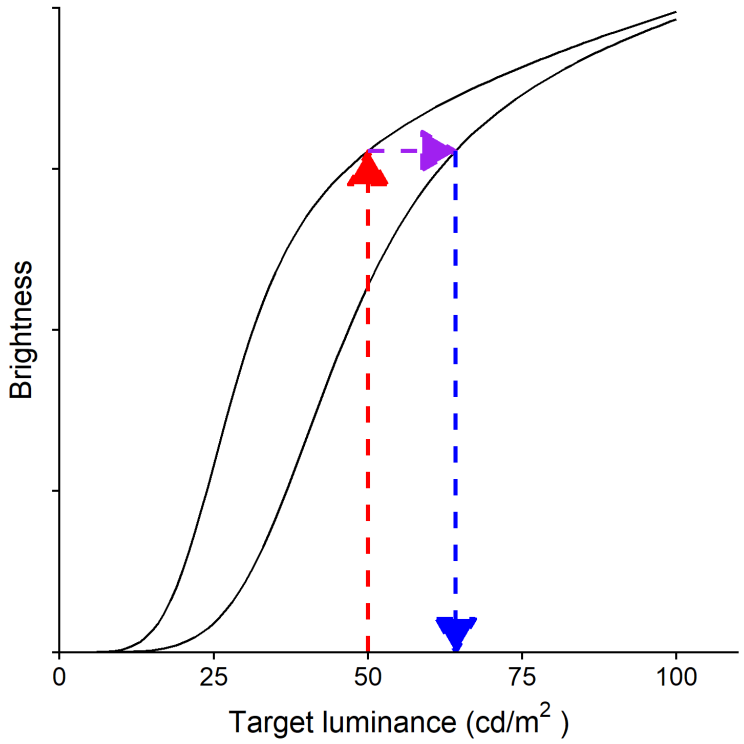

Figure 3.1: **Predicting achromatic brightness matches from LRFs** After defining an LRF for the right target, the brightness response to any physical luminance can be predicted (red arrow). Finding an equal brightness response on the LRF for the left target (purple arrow), leads to a physical luminance of the left target (blue arrow) that should be produce the same perceived brightness.

target until it has the same brightness, perceptually in the psychophysical task, or in the same arbitrary units in the model, leads to a clearly defined physical luminance of that other target that has the same brightness.

3.2 Fitting double LRF models

A combination of two LRFs, then, can predict achromatic brightness matches. To fit this model, in the least-squares sense, requires feeding in a set of physical luminance of the right target, and adjusting the parameters until the error between the predicted and actual left target luminance is minimized. The double LRF model provides several parameters that can

be adjusted to try and achieve a best fit: the translation parameter b, the scaling parameter α, the semi-saturation constant σ are the most straightforward candidates, and will be the focus of the current investigation.

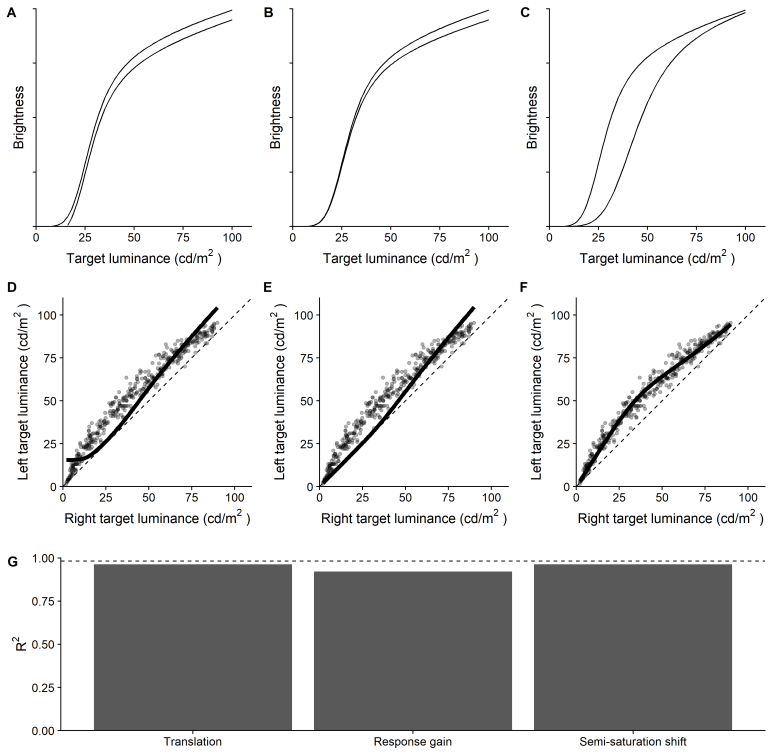

Figure 3.2: **Luminance response function based model**, and their fits, for example data from participant AGP on the Classic illusion. **A&D** Two LRFs that only differ in the horizontal position, i.e., linear translation, and the fit of this model to the exemplar data. **B&E** Two LRFs that only differ by their output scaling, i.e., linear response gain, and the fit of this model to the exemplar data. **C&F** Two LRFs that differ in their semi-saturation constant, i.e., a difference in the shape of the nonlinearity, and the fit of this model to the exemplar data. **G** Goodness-of-fit, expressed as R^2, of the three models to the exemplar data, compared to the split-half reliability (dotted line).

Figure 3.2 shows the LRF models and corresponding fits for changes in the three aforementioned parameters. The first model has two identical LRFs for the right and left targets, but the LRF for the left target has been linearly translated through the b term in equation 3.2 (Figure 3.2A). On the exemplar (participant AGP on the Classic illusion), a translation

of -.15 (arb. units) fits the data best in the least-squares sense, $R^2 = .89$. However, the scatterplot in Figure 3.2D, reveals that this model is far from adequate in capturing the data. The linear translation creates an asymptote at the lower luminance extreme, so that the left target is never predicted to be below $20\,\mathrm{cd/m^2}$. This suggest that the effect of the surround context is not to make the left target brighter by a fixed amount. The second model has the same right target LRF as the first model, but the left target LRF this time is a scaling of the right LRF, by change of the a term in equation 3.2 (Figure 3.2B). On the exemplar, a translation of .95 fits the data best in the least-squares sense, $R^2 = .87$. This is worse than the linear translation of the LRF, and the scatterplot in Figure 3.2E, reveals that this model too fails to capture the shape of the brightness matching curve. The seems to have a negligible effect below $45\,\mathrm{cd/m^2}$, where it would predict that the two targets have to be nearly the same physical luminance to match in perceived brightness. This suggest that the effect of the surround context is also not to make the left target appear brighter by a fixed ratio. The third and last model under investigation here has the same right target LRF as the first and second model. The left target LRF differs from this right target LRF by its semi-saturation constant σ in equation 3.2 (Figure 3.2C). Thus, compared to the right target, the left target has a shallower slope and reaching half-max brightness later. Since the model is fairly sensitive to this semi-saturation constant, the σ for the right LRF has also been fit to the data simultaneous with the left LRF σ. To provide a fairer comparison with the other two models (which only fit 1 parameter), the same LRF has been used for the right target for all three models. This effectively reduces all models to a 1 parameter model, with the approximately optimal parameter values for the right target LRF. Across all three models, the parameters p and q in equation 3.2 have been kept constant, at 5 and .3, respectively. On the exemplar, the semi-saturation constant for the right target LRF was fit at $\sigma = 26.14$, which was the parameter value then used for all three models. A left target LRF semi-saturation constant of $\sigma = 42.04$ fits the data best in the least-squares sense, $R^2 = .98$. This is better than both the translation and the scaling of the LRF. Figure 3.2F also reveals that this model accurately capture the full shape of the brightness matching function;

it curves close to the unity line at the more extreme luminance, and bends farther away at the intermediate luminances. Figure 3.2G presents the goodness-of-fit, expressed as R^2 for all three models. This suggests that the effect of the context is to change the shape of the nonlinear function relating physical luminance to perceived brightness of each target.

Table 3.1: **LRF model fits on the Classic illusion** for all participants.

	Reliability	Translation		Scaling		Semi-saturation		
Participant	R^2	Shift	R^2	Scalar	R^2	SS Left	SS Right	R^2
AGP	0.98	-0.15	0.89	0.95	0.87	42.04	26.14	0.98
AMC	0.98	-0.18	0.88	0.94	0.85	46.22	27.63	0.97
AYU	0.34	0.00	0.28	2.48	0.33	471.21	564.90	0.33
KXW	0.95	-0.15	0.89	0.95	0.87	46.31	31.70	0.93
MJK	0.95	-0.12	0.85	0.96	0.82	35.04	15.47	0.94
NDJ	0.95	-0.16	0.78	0.96	0.73	41.84	24.94	0.90
QXY	0.96	-0.27	0.79	0.92	0.72	51.09	22.28	0.94
RAM	0.79	-0.17	0.60	0.95	0.53	38.40	16.50	0.75
RXN	0.98	-0.15	0.93	0.95	0.93	49.81	40.85	0.97
SXF	0.97	-0.16	0.90	0.95	0.87	44.08	26.54	0.96
VXL	0.98	-0.09	0.91	0.97	0.89	31.24	16.61	0.97
YPW	0.97	-0.17	0.89	0.95	0.86	46.85	24.81	0.95
Mean	**0.90**	**-0.15**	**0.80**	**1.08**	**0.77**	**78.68**	**69.87**	**0.88**

Table 3.1 reports the best-fitting parameters, in the least-squares sense, and corresponding goodness-of-fit, expressed as R^2 for each LRF model and participant on the Classic illusion. For all participants, the model with a change in semi-saturation constants between the two models vastly outperforms the other two LRF models. Since these are not nested models, unlike the linear models, there less to be gleaned from comparing the various parameters.

Rather, Table 3.2 shows the goodness-of-fit, expressed as R^2, for each linear model and each LRF model, for each participant on the Classic illusion. With the exception of partici-

pants AYU, KXW and MJK, most achromatic brightness matching data is better explained by the LRF model based on shifted semi-saturation constants, than by any linear model.

Table 3.2: **All model fits on the Classic illusion** for all participants, in R^2 sense.

		Linear			LRF		
Participant	Reliability	Shift (+)	Scalar (x)	Both (+x)	Shift (LRF+)	Scalar (LRFx)	semi-saturation (LRFss)
AGP	0.98	0.96	0.92	0.96	0.89	0.87	0.98
AMC	0.98	0.95	0.91	0.95	0.88	0.85	0.97
AYU	0.34	0.24	0.33	0.40	0.28	0.33	0.33
KXW	0.95	0.93	0.91	0.94	0.89	0.87	0.93
MJK	0.95	0.92	0.84	0.93	0.85	0.82	0.94
NDJ	0.95	0.87	0.80	0.87	0.78	0.73	0.90
QXY	0.96	0.93	0.82	0.93	0.79	0.72	0.94
RAM	0.79	0.73	0.58	0.74	0.60	0.53	0.75
RXN	0.98	0.97	0.96	0.97	0.93	0.93	0.97
SXF	0.97	0.95	0.91	0.95	0.90	0.87	0.96
VXL	0.98	0.96	0.91	0.97	0.91	0.89	0.97
YPW	0.97	0.94	0.89	0.94	0.89	0.86	0.95
Mean	**0.90**	**0.86**	**0.81**	**0.88**	**0.80**	**0.77**	**0.88**

This can also be seen in Figure 3.3, which plots the mean goodness-of-fit, expressed as R^2 for each model, for the three stimuli. The dotted lines here indicate the ± 1 standard error of the mean reliability across observers. Notable is that all models on average perform better on the Classic illusion than on either the Checkerboard or the Radial variant. Secondly, the LRF-based models with a change in semi-saturation constant (LRFss) outperforms the other models on the Classic illusion and the Radial variant. On the Checkerboard variant, it seems to be slightly inferior to the combined linear model (+x).

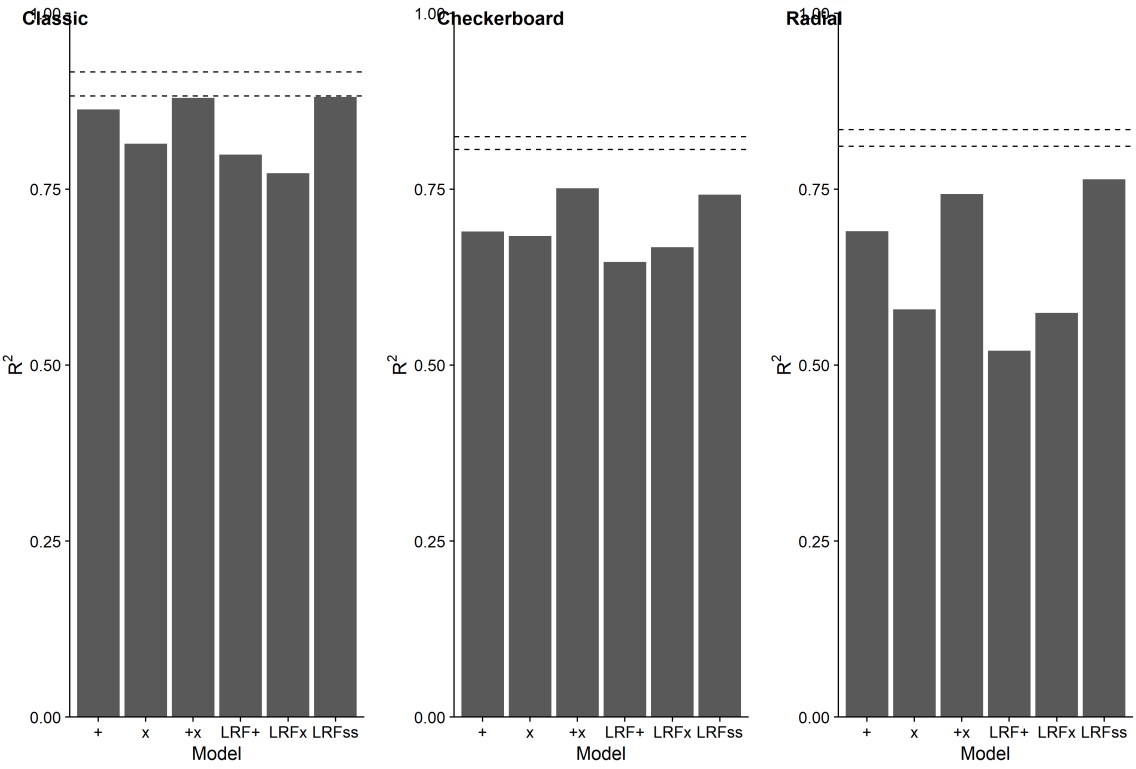

Figure 3.3: **Comparison of models**, both linear and LRF based models, for all three stimuli. The linear models consist of translation by an additive term (+), scaling (x), and both translation and scalig (+x). The LRF-based models consist of translation by an additive term (LRF+), scaling (LRFx), and different semi-saturation constants for the two LRFs (LRFss). The dotted lines here indicate the ±1 standard error of the mean reliability across observers.

Chapter 4
CONCLUSION

The achromatic brightness matching data generally follows a distinct pattern, across participants and stimuli. This suggests that this pattern could be captured mathematically, and the brightness matches thus predicted. Simple linear models are initially successful at such prediction. These linear models seem to mainly capture the approximately linear relationship between right target luminance and left target luminance at intermediate lightlevels. While these models work well across the three different stimuli, different linear transformations appeart to be important for the different stimuli; on the Classic illusion, a simple additive term translating the luminance is enough to capture most of the data. On the Checkerboard and ring variants, a scalar term provides additional predictive power. At more extreme luminance, the assumption of linear breaks down, and the linear models clearly fail to capture the induction effect at these lightlevels To overcome the limitations of the linear models, the data can be fit with a family of models derived from Luminance Response Functions. Based on the Naka-Rushton equation, these sigmoidal functions describe the relationship between a target's physical luminance and its perceived brightness. By combining two of the LRFs, brightness matches can be predicted. These LRF-based models are better at capturing the psychophysical pattern of achromatic brightness matches. Specifically, by varying the shape of the nonlinear functions through a difference semi-saturation constants, the reduced induction effect at more extreme luminances can be accurately predicted. These LRF-based models are the most effective at capturing the sorts of achromatic brightness matching data presented in the current work.

References

Adelson, E. H. (2000). Lightness Perception and Lightness Illusions. In M. Gazzaniga (Ed.), *The new cognitive neurosciences* (2nd ed., Vol. 3, pp. 339–351). Cambridge, Massachusetts.

Anderson, B. L. (1997). A theory of illusory lightness and transparency in monocular and binocular images: The role of contour junctions. *Perception*, *26*(4), 419–453. doi: 10.1068/p260419

Anderson, B. L. (2001). Contrasting theories of White's illusion. *Perception*, *30*(12), 1499–1507. doi: 10.1068/p3012ds

Anderson, B. L. (2003). Perceptual organization and White's illusion. *Perception*, *32*, 269–284.

Anderson, B. L., & Winawer, J. (2005). Image segmentation and lightness perception. *Nature*, *434*(March), 79–83. doi: 10.1038/nature03343.

Anstis, S. (2006). White's effect in lightness, color and motion. In *Seeing spatial form* (pp. 91–100).

Barkan, Y., Spitzer, H., & Einav, S. (2008). Brightness contrast-contrast induction model predicts assimilation and inverted assimilation effects. *Journal of Vision*, *8*(7), 1–26. doi: 10.1167/8.7.27

Bartleson, C. J. (1976). Brown. *Vision Research*, *1*(4), 181–191.

Berlin, B., & Kay, P. (1969). *Basic color terms: their university and evolution*. Berkeley, CA: California UP.

Betz, T., Shapley, R. M., Wichmann, F. A., & Maertens, M. (2015). Noise masking of White's illusion exposes the weakness of current spatial filtering models of lightness perception. *Journal of Vision*, *15*, 1–17. doi: 10.1167/15.14.1.doi

Blakeslee, B., & McCourt, M. E. (1999). A multiscale spatial filtering account of the White effect, simultaneous brightness contrast and grating induction. *Vision Research*, *39*, 4361–4377.

Blakeslee, B., & McCourt, M. E. (2004). A unified theory of brightness contrast and assimilation incorporating oriented multiscale spatial filtering and contrast normalization. *Vision Research*, *44*(21), 2483–2503. doi: 10.1016/j.visres.2004.05.015

Boynton, R. M., & Olson, C. X. (1990). Salience of Chromatic Basic Color Terms Confirmed by Three Measures. *Vision Research*, *30*(9), 1311–1317.

Brainard, D. H. (1997). The psychophysics toolbox. *Spatial vision*, 433–436. doi: 10.1163/156856897X00357

Bressan, P., & Kramer, P. (2008). Gating of remote effects on lightness. *Journal of Vision*, *8*(2), 1–8. doi: 10.1167/8.2.16

Buck, S. L. (2015). Brown. *Current Biology*, *25*(13), R536–R537. doi: 10.1016/j.cub.2015.05.029

Buck, S. L., & DeLawyer, T. (2012, dec). A new comparison of brown and yellow. *Journal of Vision*, *12*(14), 9. doi: 10.1167/12.14.9

Buck, S. L., & Delawyer, T. (2014). Dark vs. bright equilibrium hues: rod and cone biases. *Journal of the Optical Society of America A*, *31*(4), 1–15. doi: 10.1364/JOSAA.31.000A75

Buck, S. L., Shelton, A., Stoehr, B., Hadyanto, V., Tang, M., Morimoto, T., & DeLawyer, T. (2016). Influence of surround proximity on induction of brown and darkness. *Journal of the Optical Society of America A*, *33*(3), A12–21. doi: 10.1364/JOSAA.33.000A12

Cicerone, C. M., Volbrecht, V. J., Donnelly, S. K., & Werner, J. S. (1986). Perception of blackness. *Journal of the Optical Society of America. A, Optics and image science*, *3*(4), 432–436. doi: 10.1364/JOSAA.3.000432

Davidson, M. (1968). Perturbation approach to spatial brightness interaction in human vision. *J Opt Soc Am*, *58*(9), 1300–1308.

De Valois, R. L., & De Valois, K. K. (1993). A Multi-Stage Color Model. *Vision Research*, *33*(8), 1053–1065.

De Valois, R. L., & De Valois, K. K. (1996). On "a three-stage color model". *Vision Research*, *36*(6), 833–836. doi: 10.1016/0042-6989(96)84513-5

DeLawyer, T., Foote, K., Kwong, C., Lin, T., Short, W., Suh, E., & Buck, S. L. (2012, dec). The effects of luminance surrounds on the perception of the color brown. *Journal of Vision*, *12*(14), 36. doi: 10.1167/12.14.36

DeLawyer, T., Frederick, A., Kaplan, S., Lin, T., Shonka, T., & Buck, S. L. (2013). Dependence of the color brown on the spatial configuration of high luminance surrounds. In *presented at association for research in vision and ophthalmology.* Seattle, Washington.

DeLawyer, T., Morimoto, T., & Buck, S. L. (2016). Dichoptic perception of brown. *Journal of the Optical Society of America A*, *33*(3), A123–128. doi: 10.1364/JOSAA.33.00A123

D'Zmura, M., & Singer, B. (1999). Contrast gain control. In L. T. Sharpe & K. R. Gegenfurtner (Eds.), *Color vision: From genes to perception* (pp. 369–385). Cambridge, UK: Cambridge University Press.

Fuld, K., Werner, J. S., & Wooten, B. R. (1983). The possible elemental nature of brown. *Vision Research*, *23*(6), 631–637.

Fuld, K., Wooten, B. R., & Whalen, J. J. (1981). The elemental hues of short-wave and extraspectral lights. *Perception & Psychophysics*, *29*(4), 317–322. doi: 10.3758/BF03207340

Gilchrist, A. (2015). Theoretical approaches to lightness and perception. *Perception*, *44*(4), 339–358. doi: 10.1068/p7935

Gilchrist, A. L. (2008). Perceptual organization in lightness. In J. Wagemans (Ed.), *Oxford handbook of perceptual organization* (pp. 1–25). Oxford: Oxford University Press. doi: 10.1093/oxfordhb/9780199686858.013.031

Gilchrist, A. L. (2015). Response to Maniatis' Is a unified model of contrast and constancy possible? Reply to Gilchrist. *Vision Research*, *108*(January), 117. doi: 10.1016/j.visres.2014.12.016

Gilchrist, A. L., Kossyfidis, C., Bonato, F., Agostini, T., Cataliotti, J., Li, X., ... Economou, E. (1999). An anchoring theory of lightness perception. *Psychological review*, *106*(4), 795–834. doi: 10.1037/0033-295X.106.4.795

Graham, N. (1981). *Psychophysics of spatial-frequency channels.*

Helson, H. (1963). Studies of anomalous contrast and assimilation. *Journal of the Optical Society of America*, *53*(1), 179. doi: 10.1364/JOSA.53.000179

Helson, H., & Rohles, F. H. J. (1959). A Quantitative Study of Reversal of Classical Lightness-Contrast. *The American Journal of Psychology*, *72*(4), 530–538.

Hering, E. (1878). *Zur Lehre vom Lichtsinne*.

Hong, S. W., & Shevell, S. K. (2004a, jan). Brightness contrast and assimilation from patterned inducing backgrounds. *Vision Research*, *44*(1), 35–43. doi: 10.1016/j.visres.2003.07.010

Hong, S. W., & Shevell, S. K. (2004b). Brightness induction: unequal spatial integration with increments and decrements. *Visual Neuroscience*, *21*(3), 353–7.

Howe, P. D. L. (2005). White's effect: removing the junctions but preserving the strength of the illusion. *Perception*, *34*, 557–564. doi: 10.1068/p5414

Hurvich, L. M., & Jameson, D. (1955). Some quantitative aspects of an opponent-colors theory. II. Brightness, saturation, and hue in normal and dichromatic vision. *Journal of the Optical Society of America*, *45*(8), 602–616. doi: 10.1364/JOSA.45.000602

Hurvich, L. M., & Jameson, D. (1957). An opponent-process theory of color vision. *Psychological review*, *64, Part 1*(6), 384–404. doi: 10.1037/h0041403

Jameson, D., & Hurvich, L. M. (1955). Some Quantitative Aspects of an Opponent-Colors Theory I Chromatic Responses and Spectral Saturation. *Journal of the Optical Society of America*, *45*(7), 546. doi: 10.1364/JOSA.45.000546

Jameson, D., & Hurvich, L. M. (1975). From Contrast to Assimilation: In Art and in the Eye. *Leonardo*, *8*(2), 125–131.

Kaiser, P. K. (1971). Luminance and brightness. *Applied optics*, *10*(12), 2768–2770. doi: 10.1364/AO.10.002768

Kaneko, S., & Murakami, I. (2012). Flashed stimulation produces strong simultaneous brightness and color contrast. *Journal of vision*, *12*(12), 1–18. doi: 10.1167/12.12.1

Kiesow, F. (1930). Uber die Entstehung der Braunempfindung. *Neue Psychologische Studien*, *6*, 119–30.

Kingdom, F. A. A. (2011). Lightness, brightness and transparency: A quarter century of new ideas, captivating demonstrations and unrelenting controversy. *Vision Research*, *51*(7), 652–673. doi: 10.1016/j.visres.2010.09.012

Kulikowski, J. J. (1976). Effective contrast constancy and linearity of contrast sensation. *Vision Research*, *16*(12), 1419–1431. doi: 10.1016/0042-6989(76)90161-9

Mathworks, T. (2016). *MATLAB.*

Morimoto, T., Slezak, E., & Buck, S. L. (2016). No effects of surround complexity on brown induction. *Journal of the Optical Society of America A*, *33*(3), A45–52. doi: 10.1364/JOSAA.33.000A45

Moulden, B., & Kingdom, F. (1989). White's effect: A dual mechanism. *Vision Research*, *29*(9), 1245–1259. doi: 10.1016/0042-6989(89)90071-0

Moulden, B., & Kingdom, F. A. A. (1991). The local border mechanism in grating induction. *Vision Res*, *31*(11), 1999–2008.

Munker, H. (1970). *Abbildung auf der Netzhaut und übertragungstheoretische Beschreibung der Farbwahrnehmung* (Unpublished doctoral dissertation). Ludwig-Maximilians-Universität, München.

Naka, K. I., & Rushton, W. A. H. (1966). S-potentials from colour units in the retina of fish (Cyprinidae). *Journal of Physiology1*, *185*, 536–555.

Padgham, C. A., & Saunders, J. E. (1975). *The Perception of Light and Colour.* Academic press.

Quinn, P. C., Rosano, J. L., & Wooten, B. R. (1988, feb). Evidence that brown is not an elemental color. *Perception & Psychophysics*, *43*(2), 156–64.

Robinson, A. E., & de Sa, V. R. (2008). Brief presentations reveal the temporal dynamics of brightness induction and White's illusion. *Vision Research*, *48*(22), 2370–2381. doi: 10.1016/j.visres.2008.07.023

Robinson, A. E., Hammon, P. S., & de Sa, V. R. (2007). Explaining brightness illusions using spatial filtering and local response normalization. *Vision Research*, *47*(12), 1631–1644. doi: 10.1016/j.visres.2007.02.017

Rudd, M. E. (2013). Edge integration in achromatic color perception and the lightness darkness asymmetry. , *13*, 1–30. doi: 10.1167/13.14.18.doi

Rudd, M. E., & Arrington, K. F. (2001, dec). Darkness filling-in: a neural model of darkness induction. *Vision Research*, *41*(27), 3649–62.

Shevell, S. K. (1989). On neural signals that mediate induced blackness. *Vision Research*, *29*(7), 891–900.

Shevell, S. K., Holliday, I., & Whittle, P. (1992, dec). Two separate neural mechanisms of brightness induction. *Vision Research*, *32*(12), 2331–40.

Shinomori, K., Schefrin, B. E., & Werner, J. S. (1997). Spectral mechanisms of spatially induced blackness: data and quantitative model. *Journal of the Optical Society of America. A, Optics, image science, and vision*, *14*(2), 372–87. doi: 10.1364/JOSAA.14.000372

Singer, B., & D'Zmura, M. (1994). Color Contrast. *Vision Research*, *34*(23), 3111–3126.

Spehar, B., Clifford, C. W. G., & Agostini, T. (2002). Induction in variants of White's effect: Common or separate mechanisms? *Perception*, *31*(2), 189–196. doi: 10.1068/p10sp

Spehar, B., Gilchrist, A. L., & Arend, L. (1995). The critical role of relative luminance relations in White's effect and grating induction. *Vision Research*, *35*(18), 2603–2614. doi: 10.1016/0042-6989(95)00005-K

Todorović, D. (1997). Lightness and junctions. *Perception*, *26*, 379–394.

Todorović, D. (2010). Context effects in visual perception and their explanations. *Review of Psychology*, *17*(1), 17–32.

Uchikawa, H., Uchikawa, K., & Boynton, R. M. (1989). Influence of achromatic surrounds on categorical perception of surface colors. *Vision Research*, *29*(7), 881–890.

Vincent, J., Buck, S. L., Armer, J., Delawyer, T., & Wilson, L. (2012). Remote rings bias equilibrium brown and yellow. In *Icvs biannual meeting.* Winchester, UK.

Vincent, J., Kale, A. M., & Buck, S. L. (2016). Luminance-dependent long-term chromatic adaptation. *Journal of the Optical Society of America A*, *33*(3), A164–169. doi: 10.1364/JOSAA.33.00A164

Walker, J. T. (1978). Brightness enhancement and the Talbot level in stationary gratings. *Perception and Psychophysics*, *23*(4), 356–359. doi: 10.3758/BF03199722

Wallach, H. (1948). Brightness constancy and the nature of achromatic colors. *Journal of Experimental Psychology*, *38*(3), 310–324. doi: 10.1037/h0053804

Wesner, M. F., & Shevell, S. K. (1992). Color Perception Within a Chromatic Context: Changes in Red / Green Equilibria Caused by Noncontiguous light. *Vision Research*, *32*(9), 1623–1634.

White, M. (1979). A new effect of pattern on perceived lightness. *Perception*, *8*, 413–416.

White, M. (1981). The effect of the nature of the surround on the perceived lightness of grey bars within square-wave test gratings. *Perception*, *10*, 215–230.

White, M. (2010). The Early History of White's Illusion. *Colour: Design & Creativity*, *5*(7), 1–7.

White, M., & White, T. (1985). Counterphase lightness induction. *Vision research*, *25*(9), 1331–1335.

Yazdanbakhsh, A., Arabzadeh, E., Babadi, B., & Fazl, A. (2002). Munker-White-like illusions without T-junctions. *Perception*, *31*(6), 711–715. doi: 10.1068/p3348

Yeonan-Kim, J., & Bertalmío, M. (2016). Retinal lateral inhibition provides the biological basis of long-range spatial induction. *PLoS ONE*, *11*(12), 1–23. doi: 10.1371/journal.pone.0168963

Zaidi, Q., Spehar, B., & Shy, M. (1997). Induced effects of backgrounds and foregrounds in three-dimensional configurations: the role of T-junctions. *Perception*, *26*, 395–408.